Available online at www.sciencedirect.com
ScienceDirect
Journal of Sound and Vibration 311 (2008) 924–940
JOURNAL OF SOUND AND VIBRATION
www.elsevier.com/locate/jsvi

Analysis of nonlinear vibration of a motor–linkage mechanism system with composite links

Zhaojun Li[a,*], Ganwei Cai[a], Qibai Huang[b], Shiqing Liu[b]

[a]College of Mechanical Engineering, Guangxi University, Nanning 530004, People's Republic of China
[b]School of Mechanical Science & Engineering, Huazhong University of Science & Technology, Wuhan 430074, People's Republic of China

Received 20 August 2007; received in revised form 20 August 2007; accepted 25 September 2007
Available online 7 November 2007

Abstract

This paper studies the nonlinear vibration of a three-phase AC motor–linkage mechanism system with links fabricated from three-dimensional braided composite materials. Taking the drive motor and the linkage mechanism as an integrated system, the dynamic equations of the system are established by the finite element method. The relation between the nonlinear vibration of the system and the parameters of the system is obtained by the method of multiple scales. Results show that not only the structural parameters, but also the electromagnetic parameters and the material parameters have significant effects on the nonlinear vibration of the system. Finally, a numerical example is presented.

1. Introduction

With the use of high-speed, lightweight and high-precise mechanical transmission systems in modern industries, the investigation of the nonlinear dynamics of flexible linkage mechanisms become more and more important. Thus, many scholars have wildly studied the nonlinear dynamics of elastic linkage mechanisms by different methods for their different purposes. Chunmei et al. [1] have analyzed the nonlinear behavior of a rigid linkage mechanism with clearances through the phase portraits and Poincare maps. Seneviratne and Earles [2] have initially analyzed the nonlinear behavior of four-bar mechanism caused by joint clearances. Wang [3] has analyzed the nonlinear behavior of an elastic linkage mechanism due to the large elastic deformations of flexible links. Their studies show that there exist two main nonlinear factors in the dynamics of linkage mechanisms: one is the joint clearance of linkage mechanisms; the other is the large elastic deformation of flexible links. Although more and more researchers have paid their attention to the investigation of the nonlinear dynamics of flexible linkage mechanisms and gained some achievements [4,5], they have not taken the drive motor and the linkage mechanism as an integrated system to study.

However, some unexpected phenomena often emerge in the operation of these high-speed mechanisms. For example, these high-speed and lightweight mechanisms sometimes produce intense vibration caused by the magnetic syntony of drive motor. The main reasons are that the nonlinear vibration and coupling dynamics of

*Corresponding author.
E-mail address: glenlzj@tom.com (Z. Li).

0022-460X/$ - see front matter © 2007 Elsevier Ltd. All rights reserved.
doi:10.1016/j.jsv.2007.09.045

electromechanical systems are not studied deeply, and that the internal relation between macro-dynamic characters of electromechanical systems and electromagnetic parameters of drive motors is not discovered generally. So it is necessary to take the drive motor and the mechanism as an integrated system to study.

The three-dimensional braided fiber-reinforced composite material is an ideal material for actuating mechanism used in the high-speed mechanisms [6–8]. The purpose of this paper is to investigate the nonlinear vibration of a three-phase AC motor–linkage mechanism system with links fabricated from three-dimensional braided composites. Taking the drive motor and the mechanism as an integrated system, the dynamic equations of the system are established by the finite element method. Based on the dynamic equations of the system, the relation between the nonlinear vibration of the system and the parameters of the system is studied. Some helpful conclusions are obtained. At last, a numerical example is presented.

The diagram of the system is shown in Fig. 1. In order to simplify the discussion, the output shaft of the motor is regarded to be connected with the crank of the linkage directly.

2. Dynamic equations

2.1. Electromotor element

In the dynamic analysis of electromotor shaft, the following simplifications are employed: (1) The coupling terms of the elastic motion and the rigid body motion in the coriolis acceleration and transport acceleration are neglected in studying the absolute acceleration of any point in the shaft. (2) The effect of shearing deformation and pull–press deformation caused by transverse displacements is neglected in calculating the deformation energy. (3) Considering the lower length–diameter ratio of the electromotor rotor, it is regarded as a rigid body.

The elasticity of motor shaft is mainly taken into account in the analysis of vibration, and the shaft-disk system model is adopted in the dynamic analysis of system. The elastic motions of shaft-disk system are decided by both the eccentricity vibration of centroid of rotor, namely, the transverse vibration, and the torsional vibration of output shaft with respect to the rotor, as is shown in Fig. 2. In the diagram, numbers 1–4 denote four nodes of the element, respectively. Node 1 is set to the midpoint of the left supporting bearing, its nodal displacements are all 0; node 2 is set to the geometrical center of the electromotor rotor, and it has two nodal displacements, namely, the displacement u_1 and u_2 along the Y- and Z-axis direction, respectively; node 3, which is set to the midpoint of the right supporting bearing, has a nodal displacement u_3, namely, the angle of the torsion; node 4, which is set to the output of the shaft, has a nodal displacement u_4, namely, the angle of torsion. So the transverse vibration and the torsional vibration can be expressed by the generalized-coordinate vector $\mathbf{u}_1 = \{u_1 \quad u_2 \quad u_3 \quad u_4\}^{\mathrm{T}}$. In the diagram, XYZ is a rotating coordinate system.

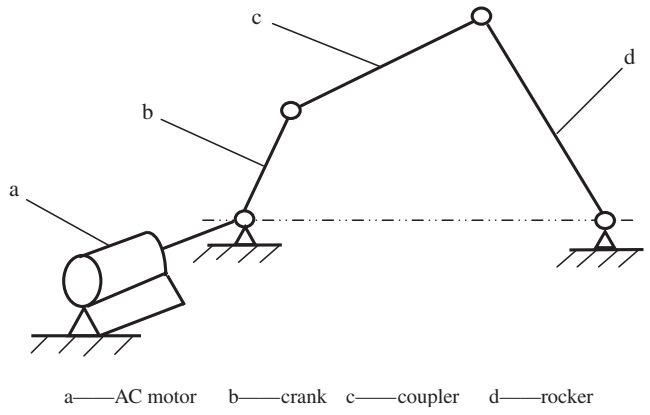

Fig. 1. Diagram of the motor–linkage mechanism system: (a) AC motor, (b) crank, (c) coupler, and (d) rocker.

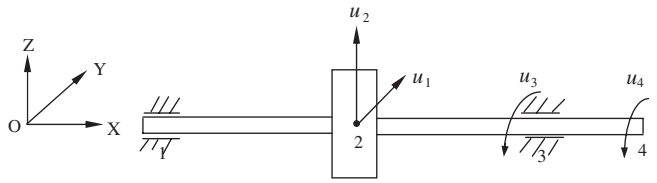

Fig. 2. Diagram of the electromotor element.

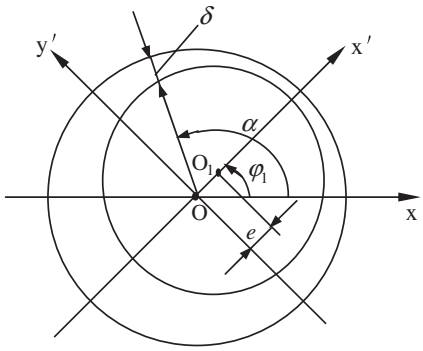

Fig. 3. Schematic diagram of air-gap eccentric vibration.

Considering the moment of inertia of the electromotor shaft (including rotor), the kinetic energy of the electromotor element can be expressed as

$$T_1 = \frac{1}{2}\int_0^{l_1} [m_1(x) + m_{10}\delta(l_{11})][\dot{W}_{1Ya}(x,t)]^2\,\mathrm{d}x + \frac{1}{2}\int_0^{l_1} [m_1(x) + m_{10}\delta(l_{11})][\dot{W}_{1Za}(x,t)]^2\,\mathrm{d}x + \frac{1}{2}\int_0^{l_1} [J_1(x) + J_{10}][\dot{V}_{1a}(x,t)]^2\,\mathrm{d}x, \tag{1}$$

where $l_1 = l_{11} + l_{12} + l_{13}$ is the length of the electromotor shaft, and l_{11}, l_{12} and l_{13} are, respectively, the length between point 1 and point 2, point 2 and point 3, point 3 and point 4; $m_1(x)$ is the mass distribution function of the electromotor shaft; m_{10} is the rotor mass which is at $x = l_{11}$; $J_1(x)$ is the moment of inertia distribution function of the electromotor shaft; J_{10} is the moment of inertia of the rotor which is at $x = l_{11}$; $\dot{W}_{1Ya}(x,t)$ is the transverse absolute velocity in the Y direction on the point of the electromotor shaft whose coordinate is x, $\dot{W}_{1Za}(x,t)$ is the transverse absolute velocity in the Z direction on the point of the electromotor shaft whose coordinate is x, $\dot{V}_{1a}(x,t)$ is the absolute angular velocity of the cross section on the electromotor shaft whose coordinated is x.

Omitting the shearing deformation energy and yield deformation energy, the elastic potential energy of the element can be written as

$$N_{11} = \frac{1}{2}\int_0^{l_1} E_1 I_1(x)\left[\frac{\partial^2 W_{1Y}(x,t)}{\partial x^2}\right]^2 \mathrm{d}x + \frac{1}{2}\int_0^{l_1} E_1 I_1(x)\left[\frac{\partial^2 W_{1Z}(x,t)}{\partial x^2}\right]^2 \mathrm{d}x + \frac{1}{2}\int_0^{l_1} G_1 J_{01}(x)\left[\frac{\partial V_1(x,t)}{\partial x}\right]^2 \mathrm{d}x, \tag{2}$$

where $W_{1Y}(x,t)$ is the transverse displacement in the Y direction on the point of the electromotor shaft whose coordinate is x, $W_{1Z}(x,t)$ is the transverse displacement in the Z direction on the point of the electromotor shaft whose coordinate is x, $V_1(x,t)$ is the angle of elastic torsion on the point of the electromotor shaft whose coordinate is x (see Appendix); E_1 is the Young's modulus of the electromotor shaft material; G_1 is the shear elastic modulus of the electromotor shaft material; $I_1(x)$ is the distribution function of the anti-bending sectional moment of inertia of the electromotor; $J_{01}(x)$ is the distribution function of the polar moment of inertia of the electromotor.

The air-gap eccentric vibration of the rotor is shown in Fig. 3, where point O is the inner circle geometric center of the stator, point O_1 is the outer circle geometric center of the rotor and its coordinate is (u_1, u_2), δ is the length of air gap, e is the air-gap eccentricity and

$$e = \sqrt{u_1^2 + u_2^2}. \tag{3}$$

According to electromechanical analysis dynamics, the air-gap magnetic energy of the electromotor can be written as [9]

$$N_{12} = \frac{R_1 L_{01}}{2} \int_0^{2\pi} \Lambda_0 \sum_{n=0}^{\infty} \varepsilon_1^n \cos^n(\alpha - \varphi_1)\left[F_{1m}\cos(\omega_0 t - \alpha) + F_{2m}\cos(\varphi_1 + s\omega_0 t - \alpha - \phi)\right]^2 \mathrm{d}\alpha, \tag{4}$$

where R_1 is the inner radius of the electromotor stator; L_{01} is the effective length of the rotor; $\Lambda_0 = \mu_0/\sigma$, is the even air-gap permeance of the electromotor, $\sigma = k_\mu \delta_0$, μ_0 is the magnetic permeability coefficient of air, k_μ is saturation, $k_\mu = 1 + \delta_{\mathrm{Fe}}/k_1\delta_0$, k_1 is the calculation air-gap coefficient of the even air gap, δ_{Fe} is the equivalent air-gap of ferromagnetic materials; $\varepsilon_1 = e/k_\mu\delta_0$, is the effective relative eccentricity; $\omega_0 = 60f/p$, is the synchronous speed of electromotor, f is the frequency of power, p is the number of magnetic pole-pair of the compounded magnetic field; s is the slide ratio; φ_1 is the rotation angle of the crank; ϕ is the phase angle of rotor current lagging behind the stator current; F_{1m} and F_{2m} are the three-phase compounded magnetomotive amplitude of the stator and rotor, respectively.

The total potential energy N_1 of the element contains the elastic potential energy N_{11} and the air-gap magnetic energy of electromotor N_{12}, namely

$$N_1 = N_{11} + N_{12}. \tag{5}$$

Lagrange equation which is used in the electromotor element can be expressed as

$$\frac{\mathrm{d}}{\mathrm{d}t}\left(\frac{\partial T_1}{\partial \dot{\mathbf{u}}_1}\right) - \frac{\partial T_1}{\partial \mathbf{u}_1} + \frac{\partial N_1}{\partial \mathbf{u}_1} = \bar{\mathbf{f}}_1 + \bar{\mathbf{q}}_1, \tag{6}$$

where $\bar{\mathbf{f}}_1$ is the external excitation force vector, $\bar{\mathbf{q}}_1$ is the force vector exerted on the electromotor element by the other elements connecting to the electromotor element.

Substituting Eqs. (1)–(5) into Eq. (6), rearranging, and omitting the effect of the damping, the dynamic equation of the electromotor element is obtained as

$$\bar{\mathbf{m}}_1\ddot{\mathbf{u}}_1 + (\bar{\mathbf{k}}_1 + \bar{\mathbf{k}}_{01})\mathbf{u}_1 = \bar{\mathbf{f}}_1 + \bar{\mathbf{q}}_1 - \bar{\mathbf{m}}_1\ddot{\mathbf{u}}_{1r}, \tag{7}$$

where $\bar{\mathbf{m}}_1$ is the mass matrix of the electromotor element, $\bar{\mathbf{k}}_1$ is the stiffness matrix of the electromotor element related to N_{11}, $\bar{\mathbf{k}}_{01}$ is the stiffness matrix of the electromotor element related to N_{12} (see the Appendix); $\ddot{\mathbf{u}}_{1r}$ is the rigid body acceleration vector of the electromotor element.

2.2. Beam element of three-dimensional braided composite materials

The basic fiber structure of the three-dimensional braided composite materials is of three-dimensional and four-directional texture, as is shown in Fig. 4 [6], and the geometrical unit-cell can be adopted in analysis, as is shown in Fig. 5 [7]. Four bundles of braided yarns are in the diagonal direction of the unit-cell, and intersect at the center point O. Each braided yarn makes an angle α with x-axis, called the braided angle, and its projection in the y–z plane makes an angle β with y-axis. As is shown in Fig. 4, the α and β belong to the first direction braided yarn. By analyzing the stiffness characteristic of this material by the laminated plate analogy, the materials can be regarded as the superposition of four unidirectional fiber composite materials, and the stiffness of the materials is the superposition of stiffness of the four parts according to their volume fractions [8].

In general, the links of the linkage mechanism are slim bars, so the links fabricated from three-dimensional braided composites can be simulated using the beam element.

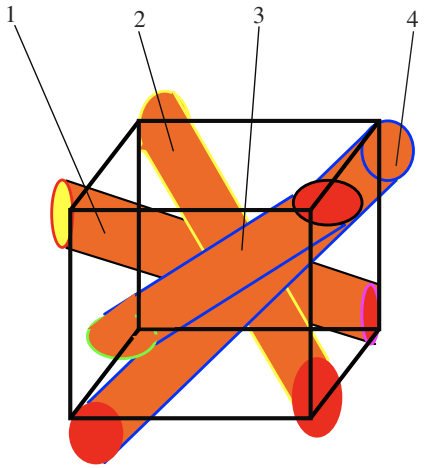

Fig. 4. Three-dimensional and four-directional structure of the three-dimensional braided composite material.

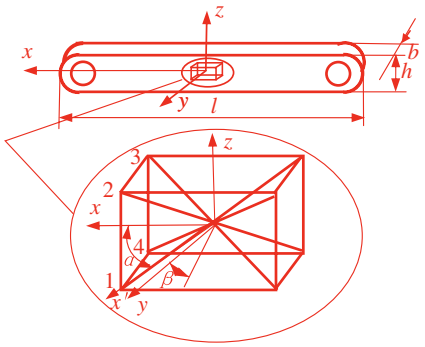

Fig. 5. Geometrical unit cell.

According to the finite element method, the generalized-coordinate vector of the beam element of three-dimensional braided composite materials can be expressed as

$$\mathbf{u}_2 = \{u_5 \quad u_6 \quad u_7 \quad u_8 \quad u_9 \quad u_{10} \quad u_{11} \quad u_{12}\}^{\mathrm{T}},$$

where u_5 and u_9 are the longitudinal displacements of the nodes, u_6 and u_{10} are the transverse displacements of the nodes, u_7 and u_{11} are the elastic rotation angles of axes at the nodes, u_8 and u_{12} are the curvatures of axes at the nodes.

The kinetic energy of the beam element can be expressed as

$$T_2 = \frac{1}{2}\int_0^{l_2} m_2(\bar{x})\,[\dot{W}_{2a}(\bar{x},t)]^2\,\mathrm{d}\bar{x} + \frac{1}{2}\int_0^{l_2} m_2(\bar{x})\,[\dot{V}_{2a}(\bar{x},t)]^2\,\mathrm{d}\bar{x}, \tag{8}$$

where $\bar{x}$ is the coordinate of the beam element in the local coordinate system; l_2 is the length of the beam element; $m_2(\bar{x})$ is the mass distribution function of the beam element, $m_2(\bar{x}) = \rho_2 A_2(\bar{x})$, ρ_2 is the average mass density of materials, $\rho_2 = \rho_{2f} v_{2f} + \rho_{2m} v_{2m}$, ρ_{2f} and ρ_{2m} are the densities of fiber and matrix, respectively, v_{2f} and v_{2m} are the volume ratio of fiber and matrix, respectively, $A_2(\bar{x})$ is the distribution function of the area of the cross-section of the beam element; $\dot{W}_{2a}(\bar{x},t)$ is the transverse absolute velocity of the central point of any cross section of the element; $\dot{V}_{2a}(\bar{x},t)$ is the longitudinal absolute velocity of the central point of any cross section of the element; $W_2(\bar{x},t)$ is the transverse displacement of the central point of any cross section of the element, $V_2(\bar{x},t)$ is the longitudinal displacement of the central point of any cross section of the element (see the Appendix).

According to microstructure of composite materials, the strain energy of the jth part in the beam element can be expressed as

$$N_{2j} = \frac{1}{2}\int_{\Omega_j} \varepsilon_{2j}^{\mathrm{T}} \sigma_{2j}\, \mathrm{d}\Omega_j, \tag{9}$$

where Ω_j is the volume of the jth part; $\boldsymbol{\varepsilon}_{2j}$ and $\boldsymbol{\sigma}_{2j}$ are, respectively, the strain and stress vectors of the jth part in its orthogonal axis coordinate system $x'y'z'$.

Each part can be considered as transverse isotropic, so the constitutive relation of the jth part in its orthogonal axis coordinate system $x'y'z'$ can be expressed as [8]

$$\boldsymbol{\sigma}_{2j} = \mathbf{C}_{2j}\boldsymbol{\varepsilon}_{2j}, \tag{10}$$

where

$$\mathbf{C}_{2j} = \begin{pmatrix} C_{11} & C_{12} & C_{13} & & & \\ C_{12} & C_{22} & C_{23} & & 0 & \\ C_{13} & C_{23} & C_{33} & & & \\ & & & C_{44} & & \\ & 0 & & & C_{55} & \\ & & & & & C_{66} \end{pmatrix},$$

$$\begin{aligned} &C_{11} = (1-\mu_{23}\mu_{23})E_{11}/K, && C_{12} = (1+\mu_{23})\mu_{21}E_{11}/K,\\ &C_{22} = C_{33} = (1-\mu_{21}\mu_{12})E_{22}/K, && C_{23} = (\mu_{23}+\mu_{12}\mu_{21})E_{22}/K,\\ &C_{44} = G_{23}; C_{55} = G_{13}; C_{66} = G_{12}, && K = 1-2\mu_{12}\mu_{21}(1+\mu_{23})-\mu_{23}\mu_{23} \end{aligned}$$

according to micromechanics of composite materials, the elastic constants E_{ij}, G_{ij} and μ_{ij} can be calculated from elastic constants of fiber and matrix, volume ratio of fiber and the microstructure parameters of composite materials.

The strain vector of the jth part in the beam coordinate system xyz can be obtained from the transition relation of strain in elastic mechanics as

$$\boldsymbol{\varepsilon}_{2j} = \mathbf{L}_{2j}\boldsymbol{\varepsilon}_2, \tag{11}$$

where $\mathbf{L}_{2j}$ is the transition matrix of strain which is determined by the direction cosine between the beam coordinate system xyz and the orthogonal axis coordinate system $z'y'z'$ of the jth part; $\boldsymbol{\varepsilon}_2$ is the strain vector of the beam element.

The relation between the strains and nodal displacements can be written as [8]

$$\boldsymbol{\varepsilon}_2 = \mathbf{S}_2\mathbf{u}_2, \tag{12}$$

where

$$\mathbf{S}_2 = [\mathbf{S}_{21} \quad \mathbf{S}_{22} \quad \mathbf{S}_{23} \quad \mathbf{S}_{24} \quad \mathbf{S}_{25} \quad \mathbf{S}_{26}]^{\mathrm{T}},$$

$$\mathbf{S}_{21} = \{\phi_5'(\bar{x}) \quad 0 \quad 0 \quad 0 \quad \phi_9'(\bar{x}) \quad 0 \quad 0 \quad 0\}^{\mathrm{T}},$$

$$\mathbf{S}_{25} = \{0 \quad \phi_6'(\bar{x}) \quad \phi_7'(\bar{x}) \quad \phi_8'(\bar{x}) \quad 0 \quad \phi_{10}'(\bar{x}) \quad \phi_{11}'(\bar{x}) \quad \phi_{12}'(\bar{x})\}^{\mathrm{T}},$$

$$\mathbf{S}_{22} = \mathbf{S}_{23} = \mathbf{S}_{24} = \mathbf{S}_{26} = \{0 \quad 0 \quad 0 \quad 0 \quad 0 \quad 0 \quad 0 \quad 0\}^{\mathrm{T}}.$$

Substituting Eqs. (10)–(12) into Eq. (9), rearranging, the following equation can be obtained as

$$N_{2j} = \mathbf{u}_2^{\mathrm{T}}\left(\frac{1}{2}\int_{\Omega_j} \mathbf{S}_2^{\mathrm{T}}\mathbf{L}_{2j}^{\mathrm{T}}\mathbf{C}_{2j}\mathbf{L}_{2j}\mathbf{S}_2\, \mathrm{d}\Omega_j\right)\mathbf{u}_2. \tag{13}$$

As described above, the three-dimensional braided composite materials can be regarded as the superposition of four unidirectional fiber composite materials, so the total potential energy of the beam element is

$$N_2 = \mathbf{u}_2^{\mathrm{T}}\left(\sum_{j=1}^{4}\frac{1}{2}\int_{\Omega_j}\mathbf{S}_2^{\mathrm{T}}\mathbf{L}_{2j}^{\mathrm{T}}\mathbf{C}_{2j}\mathbf{L}_{2j}\mathbf{S}_2\,\mathrm{d}\Omega_j\right)\mathbf{u}_2. \tag{14}$$

Lagrange equation which is used in the beam element of three-dimensional braided composite materials can be expressed as

$$\frac{\mathrm{d}}{\mathrm{d}t}\left(\frac{\partial T_2}{\partial \dot{u}_2}\right) - \frac{\partial T_2}{\partial u_2} + \frac{\partial N_2}{\partial u_2} = \bar{\mathbf{f}}_2 + \bar{\mathbf{q}}_2, \tag{15}$$

where $\bar{\mathbf{f}}_2$ is the external excitation force vector, $\bar{\mathbf{q}}_2$ is the force vector exerted on the beam element by the other elements connecting to the beam element.

Substituting Eqs. (8) and (14) into Eq. (15), rearranging, and omitting the effect of the damping, the dynamic equation of the beam element of three-dimensional braided composite materials is obtained as

$$\bar{\mathbf{m}}_2\ddot{\mathbf{u}}_2 + \bar{\mathbf{k}}_2\mathbf{u}_2 = \bar{\mathbf{f}}_2 + \bar{\mathbf{q}}_2 - \bar{\mathbf{m}}_2\ddot{\mathbf{u}}_{2r}, \tag{16}$$

where $\bar{\mathbf{m}}_2$ is the mass matrix of the beam element, $\bar{\mathbf{k}}_2$ is the stiffness matrix of the beam element (see the Appendix); $\ddot{\mathbf{u}}_{2r}$ is the rigid body acceleration vector of the beam element.

2.3. Dynamic equations

In order to simplify the problems and make the leading issues prominent, the three-phase AC motor–linkage mechanism system with links fabricated from three-dimensional braided composites is divided into six elements. The electromotor is regarded as one element, as shown in Fig. 6. The crank is regarded as one beam element, and the coupler and the rocker are, respectively, divided into two beam elements, as shown in Fig. 7. The serial numbers of the nodes are represented by 1, 2, …. The serial numbers of the elements are represented by ①, ②, …. The serial numbers of the links are represented by (1), (2), …. U_1, U_2, U_7, U_8, U_{11}, U_{12}, U_{15}, U_{16}, U_{19}, U_{20} are the elastic displacements; U_5, U_9, U_{10}, U_{13}, U_{17}, U_{18}, U_{21}, U_{23} are the elastic rotation angles; U_3, U_4 are the torsion angles; U_6, U_{14}, U_{22}, U_{24} are the curvatures. So the elastic displacement vector of the system in the global coordinates is

$$\begin{aligned}\mathbf{U} = \{&U_1 \quad U_2 \quad U_3 \quad U_4 \quad U_5 \quad U_6 \quad U_7 \quad U_8 \quad U_9 \quad U_{10} \quad U_{11} \quad U_{12} \quad U_{13}\\ &U_{14} \quad U_{15} \quad U_{16} \quad U_{17} \quad U_{18} \quad U_{19} \quad U_{20} \quad U_{21} \quad U_{22} \quad U_{23} \quad U_{24}\}^{\mathrm{T}}.\end{aligned}$$

Assuming that $\mathbf{R}_i$ is the transformation matrix of the ith element between the element coordinates and the global coordinates, and $\mathbf{B}_i$ is the coordinate compatible matrix of the ith element between the local number and the global number, the dynamic equation of the element ① in the global coordinates can be expressed as

$$\mathbf{M}_1^e\ddot{\mathbf{U}} + (\mathbf{K}_1^e + \mathbf{K}_{01}^e)\mathbf{U} = \mathbf{F}_1^e + \mathbf{Q}_1^e - \mathbf{M}_1^e\ddot{\mathbf{U}}_r, \tag{17}$$

where $\mathbf{U}$, $\ddot{\mathbf{U}}$, $\ddot{\mathbf{U}}_r$, respectively, represent the elastic displacement vector, the acceleration vector and the rigid body acceleration vector of the system in the global coordinates, and

$$\mathbf{M}_1^e = \mathbf{B}_1^{\mathrm{T}}\mathbf{R}_1^{\mathrm{T}}\bar{\mathbf{m}}_1\mathbf{R}_1\mathbf{B}_1, \quad \mathbf{K}_1^e = \mathbf{B}_1^{\mathrm{T}}\mathbf{R}_1^{\mathrm{T}}\bar{\mathbf{k}}_1\mathbf{R}_1\mathbf{B}_1, \quad \mathbf{K}_{01}^e = \mathbf{B}_1^{\mathrm{T}}\mathbf{R}_1^{\mathrm{T}}\bar{\mathbf{k}}_{01}\mathbf{R}_1\mathbf{B}_1,$$

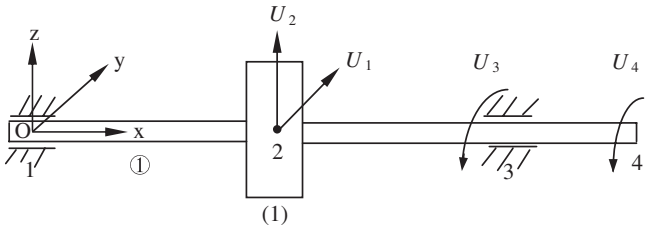

Fig. 6. Electromotor element.

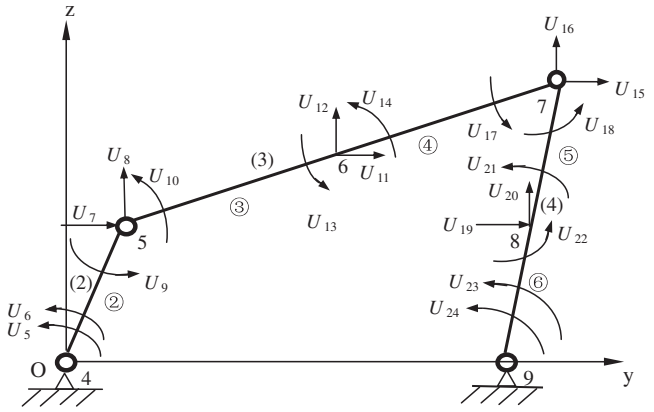

Fig. 7. Elastic linkage mechanism.

$$\mathbf{F}_1^e = \mathbf{B}_1^{\mathrm{T}}\mathbf{R}_1^{\mathrm{T}}\bar{\mathbf{f}}_1, \quad \mathbf{Q}_1^e = \mathbf{B}_1^{\mathrm{T}}\mathbf{R}_1^{\mathrm{T}}\bar{\mathbf{q}}_1.$$

The dynamic equation of the ith element in the global coordinates can be expressed as

$$\mathbf{M}_i^e\ddot{\mathbf{U}} + \mathbf{K}_i^e\mathbf{U} = \mathbf{F}_i^e + \mathbf{Q}_i^e - \mathbf{M}_i^e\ddot{\mathbf{U}}_r, \tag{18}$$

where $i = 2, 3, 4, 5, 6$, and

$$\mathbf{M}_i^e = \mathbf{B}_i^{\mathrm{T}}\mathbf{R}_i^{\mathrm{T}}\bar{\mathbf{m}}_2\mathbf{R}_i\mathbf{B}_i, \quad \mathbf{K}_i^e = \mathbf{B}_i^{\mathrm{T}}\mathbf{R}_i^{\mathrm{T}}\bar{\mathbf{k}}_2\mathbf{R}_i\mathbf{B}_i, \quad \mathbf{F}_i^e = \mathbf{B}_i^{\mathrm{T}}\mathbf{R}_i^{\mathrm{T}}\bar{\mathbf{f}}_2, \quad \mathbf{Q}_i^e = \mathbf{B}_i^{\mathrm{T}}\mathbf{R}_i^{\mathrm{T}}\bar{\mathbf{q}}_2.$$

Without consideration of the effect of the damping of the system by Eqs. (17) and (18), the dynamic equation of the system can be obtained as

$$\mathbf{M}\ddot{\mathbf{U}} + (\mathbf{K} + \mathbf{K}_{01})\mathbf{U} = \mathbf{F} - \mathbf{M}\ddot{\mathbf{U}}_r, \tag{19}$$

where

$$\mathbf{M} = \sum_{i=1}^{6}\mathbf{M}_i^e, \quad \mathbf{K} = \sum_{i=1}^{6}\mathbf{K}_i^e, \quad \mathbf{K}_{01} = \mathbf{K}_{01}^e, \quad \mathbf{F} = \sum_{i=1}^{6}\mathbf{F}_i^e.$$

Assuming that the damping changes with elastic distortion in direct ratio, and considering the effect of the damping of system, the dynamic equation of the motor–elastic linkage mechanism system with links fabricated from three-dimensional braided composites is

$$\mathbf{M}\ddot{\mathbf{U}} + \mathbf{C}\dot{\mathbf{U}} + (\mathbf{K} + \mathbf{K}_{01})\mathbf{U} = \mathbf{F} - \mathbf{M}\ddot{\mathbf{U}}_r, \tag{20}$$

where $\mathbf{C}$ is the damping matrix of the system.

3. Analysis of nonlinear vibration

According to electromechanical dynamics, the dynamic equation of the electromotor shaft, which is rotating around its fixed axis, can be written as

$$J_0\ddot{\varphi}_1 = T_e - T_{\mathrm{Cu}} - T_r - T_0, \tag{21}$$

where J_0 is the moment of inertial of the electromotor shaft, including the moment of inertia of the rotor J_{10}; T_e is the electromagnetic torque of the electromotor; T_{Cu} is the copper loss torque of the electromotor; T_r is the load torque of the electromotor; T_0 is the runaway braking torque of the electromotor, which is much smaller than T_r.

According to electromechanical dynamics, T_e can be written as

$$T_e = \frac{\partial N_{12}}{\partial \varphi_1}. \tag{22}$$

Substituting Eq. (4) into Eq. (22), and rearranging, T_e is obtained as

$$T_e = \frac{g_1}{J_0} + \frac{g_1}{2\sigma^2 J_0}(U_1^2 + U_2^2) - \left[\frac{g_2}{4\sigma^2 J_0}(U_1^2 - U_2^2) - \frac{g_3}{2\sigma^2} U_1 U_2\right] \sin(\Omega_0 t) + \left[\frac{g_3}{4\sigma^2 J_0}(U_1^2 - U_2^2) + \frac{g_2}{2\sigma^2 J_0} U_1 U_2\right] \cos(\Omega_0 t), \tag{23}$$

where U_1, U_2 are, respectively, the first and second coordinates which represent the elastic displacement of the electromotor shaft, as shown in Fig. 6,

$$g_1 = \pi R L_0 \Lambda_0 F_{1m} F_{2m} \sin\phi,$$

$$g_2 = \pi R L_0 \Lambda_0 (F_{1m} F_{2m} \cos\phi + F_{2m}^2 \cos 2\phi),$$

$$g_3 = \pi R L_0 \Lambda_0 (F_{1m} F_{2m} \sin\phi + F_{2m}^2 \sin 2\phi)$$

and

$$\Omega_0 = 2\omega_0. \tag{24}$$

According to electromechanical dynamics, T_{Cu} can be written as

$$T_{\mathrm{Cu}} = sT_e, \tag{25}$$

where s is the slip ratio.

According to mechanics of materials, T_r can be written as

$$T_r = E_2 I_2 U_6, \tag{26}$$

where E_2 is the Young's modulus of the material of the crank, I_2 is the moment of inertial of the root of the crank, U_6 is the sixth coordinate which represents the curvature of the crank, as shown in Fig. 7.

Substituting Eqs. (23), (25), (26) into Eq. (21), omitting T_0, and rearranging, the following equation can be given:

$$\ddot{\varphi}_1 = -\frac{E_2 I_2}{J_0} U_6 + \varepsilon\left\{\frac{(1-s)g_1}{2\sigma^2 J_0}(U_1^2 + U_2^2) + (1-s)\left[\frac{g_3}{4\sigma^2 J_0}(U_1^2 - U_2^2) + \frac{g_2}{2\sigma^2 J_0} U_1 U_2\right] \cos(\Omega_0 t) - (1-s)\left[\frac{g_2}{4\sigma^2 J_0}(U_1^2 - U_2^2) - \frac{g_3}{2\sigma^2} U_1 U_2\right] \sin(\Omega_0 t)\right\}. \tag{27}$$

Replacing U_1, U_2 and U_6 by $\mathbf{U}$, and rearranging, Eq. (27) can be written as

$$\ddot{\varphi}_1 = \mathbf{U}_{\varepsilon 1}^{\mathrm{T}} \mathbf{U} + \mathbf{U}^{\mathrm{T}} \mathbf{K}_{\varepsilon 1} \mathbf{U} + \mathbf{U}^{\mathrm{T}} \mathbf{K}_{\varepsilon 2} \mathbf{U} \cos(\Omega_0 t) + \mathbf{U}^{\mathrm{T}} \mathbf{K}_{\varepsilon 3} \mathbf{U} \sin(\Omega_0 t), \tag{28}$$

where $\mathbf{K}_{\varepsilon 1}$, $\mathbf{K}_{\varepsilon 2}$, $\mathbf{K}_{\varepsilon 3}$ are the 24th-order matrixes, $\mathbf{U}_{\varepsilon 1}$ is the 24th-order vector, and

$$(\mathbf{U}_{\varepsilon 1})_6 = -\frac{E_2 I_2}{J_0}, \quad (\mathbf{K}_{\varepsilon 1})_{11} = (\mathbf{K}_{\varepsilon 1})_{22} = \frac{(1-s)g_1}{2\sigma^2 J_0},$$

$$(\mathbf{K}_{\varepsilon 2})_{11} = \frac{(1-s)g_3}{4\sigma^2 J_0}, \quad (\mathbf{K}_{\varepsilon 2})_{22} = -\frac{(1-s)g_3}{4\sigma^2 J_0}, \quad (\mathbf{K}_{\varepsilon 2})_{21} = (\mathbf{K}_{\varepsilon 2})_{12} = \frac{(1-s)g_2}{2\sigma^2 J_0},$$

$$(\mathbf{K}_{\varepsilon 3})_{11} = -\frac{(1-s)g_3}{4\sigma^2 J_0}, \quad (\mathbf{K}_{\varepsilon 3})_{22} = \frac{(1-s)g_3}{4\sigma^2 J_0}, \quad (\mathbf{K}_{\varepsilon 3})_{21} = (\mathbf{K}_{\varepsilon 3})_{12} = \frac{(1-s)g_2}{2\sigma^2 J_0},$$

the other terms of $\mathbf{U}_{\varepsilon 1}$, $\mathbf{K}_{\varepsilon 1}$, $\mathbf{K}_{\varepsilon 2}$, $\mathbf{K}_{\varepsilon 3}$ are all zero.

The self-excitation inertia force of the system can be represented as

$$\mathbf{Q} = -\mathbf{M}\ddot{\mathbf{U}}_r, \tag{29}$$

where $\ddot{\mathbf{U}}_r$ is the rigid body acceleration vector of the system in the global coordinates.

According to mechanisms, $\ddot{\mathbf{U}}_r$ can be expressed as [10]

$$\ddot{\mathbf{U}}_r = \mathbf{U}_\omega \dot{\varphi}_1^2 + \mathbf{U}_\varepsilon \ddot{\varphi}_1, \tag{30}$$

where $\mathbf{U}_\omega$ and $\mathbf{U}_\varepsilon$ are the 24th-order coefficient vectors which are determined by the structural parameters of the system.

Substituting Eqs. (28) and (30) into Eq. (29), expanding the parts of the self-excitation inertia force which is related to $\dot{\varphi}_1^2$ into Fourier series, and rearranging, the following equation can be given:

$$\begin{aligned}\mathbf{Q} = &\sum_{k=1}^{N} \mathbf{F}_{Dk} - \mathbf{M}\mathbf{U}_\varepsilon \mathbf{U}_{\varepsilon 1}^{\mathrm{T}} \mathbf{U} - \mathbf{M}\mathbf{U}_\varepsilon \mathbf{U}^{\mathrm{T}} \mathbf{K}_{\varepsilon 1} \mathbf{U} \\ &- \mathbf{M}\mathbf{U}_\varepsilon \mathbf{U}^{\mathrm{T}} \mathbf{K}_{\varepsilon 2} \mathbf{U} \cos(\Omega_0 t) - \mathbf{M}\mathbf{U}_\varepsilon \mathbf{U}^{\mathrm{T}} \mathbf{K}_{\varepsilon 3} \mathbf{U} \sin(\Omega_0 t),\end{aligned} \tag{31}$$

where N and $\mathbf{F}_{Dk}$ are, respectively, the maximum selected term number and vector of the k-order term of the expansion of the Fourier series, and $\mathbf{F}_{Dk}$ is expressed as

$$(\mathbf{F}_{Dk})_i = \mathbf{F}_{Dki} \cos(k\Omega_1 t + \varphi_{ki}), \tag{32}$$

where Ω_i is the rotating speed of rotor, F_{Dki} and φ_{ki} are, respectively, the amplitude and phase angle, which can be obtained by the expansion of Fourier series.

According to the derivation of Eq. (20), $\mathbf{K}_{01}$ is determined by the electromagnetic parameters of the motor, and it can be expressed as

$$\mathbf{K}_{01} = \mathbf{K}_{11} + \mathbf{K}_{12} \cos(\Omega_0 t) + \mathbf{K}_{13} \sin(\Omega_0 t), \tag{33}$$

where $\mathbf{K}_{11}$, $\mathbf{K}_{12}$, $\mathbf{K}_{13}$ are all the 24th-order matrices (see the Appendix).

Without consideration of the external excitation force $\mathbf{F}$, substituting Eqs. (29), (31) and (33) into Eq. (20), introducing ε as the designator for these small quantities, and rearranging, the following equation can be given:

$$\begin{aligned}\mathbf{M}\ddot{\mathbf{U}} + \mathbf{K}\mathbf{U} = &\sum_{k=1}^{N} \mathbf{F}_{Dk} + \varepsilon[-\mathbf{M}\mathbf{U}_\varepsilon \mathbf{U}_{\varepsilon 1}^{\mathrm{T}} \mathbf{U} - \mathbf{M}\mathbf{U}_\varepsilon \mathbf{U}^{\mathrm{T}} \mathbf{K}_{\varepsilon 1} \mathbf{U} \\ &- \mathbf{M}\mathbf{U}_\varepsilon \mathbf{U}^{\mathrm{T}} \mathbf{K}_{\varepsilon 2} \mathbf{U} \cos(\Omega_0 t) - \mathbf{M}\mathbf{U}_\varepsilon \mathbf{U}^{\mathrm{T}} \mathbf{K}_{\varepsilon 3} \mathbf{U} \sin(\Omega_0 t) \\ &- \mathbf{K}_{11}\mathbf{U} - \mathbf{K}_{12}\mathbf{U} \cos(\Omega_0 t) - \mathbf{K}_{13}\mathbf{U} \sin(\Omega_0 t) - \mathbf{C}\dot{\mathbf{U}}].\end{aligned} \tag{34}$$

Eq. (34) shows that the dynamic equation of the motor–elastic linkage mechanism system with links fabricated from three-dimensional braided composites is nonlinear.

Assuming that the linear transfer functions are:

$$\begin{cases} \mathbf{U} = \boldsymbol{\phi}\boldsymbol{\eta}, \\ \dot{\mathbf{U}} = \boldsymbol{\phi}\dot{\boldsymbol{\eta}}, \\ \ddot{\mathbf{U}} = \boldsymbol{\phi}\ddot{\boldsymbol{\eta}}, \end{cases} \tag{35}$$

where $\boldsymbol{\phi}$ is the modal transfer matrix, $\boldsymbol{\eta}$ is the modal coordinate vector corresponding to $\boldsymbol{\phi}$.

Substituting Eq. (35) into Eq. (34), multiplying the equation by $\boldsymbol{\phi}^{\mathrm{T}}$, and rearranging, the following equation can be given:

$$\begin{aligned}\ddot{\boldsymbol{\eta}} + \mathbf{K}_0\boldsymbol{\eta} = &\sum_{k=1}^{N} \mathbf{F}_{0Dk} + \varepsilon[-\boldsymbol{\phi}^{\mathrm{T}}\mathbf{M}\mathbf{U}_\varepsilon \mathbf{U}_{\varepsilon 1}^{\mathrm{T}} \boldsymbol{\phi}\boldsymbol{\eta} - \boldsymbol{\phi}^{\mathrm{T}}\mathbf{M}\mathbf{U}_\varepsilon \boldsymbol{\eta}^{\mathrm{T}} \mathbf{K}_{0\varepsilon 1}\boldsymbol{\eta} \\ &- \boldsymbol{\phi}^{\mathrm{T}}\mathbf{M}\mathbf{U}_\varepsilon \boldsymbol{\eta}^{\mathrm{T}} \mathbf{K}_{0\varepsilon 2}\boldsymbol{\eta} \cos(\Omega_0 t) - \boldsymbol{\phi}^{\mathrm{T}}\mathbf{M}\mathbf{U}_\varepsilon \boldsymbol{\eta}^{\mathrm{T}} \mathbf{K}_{0\varepsilon 3}\boldsymbol{\eta} \sin(\Omega_0 t) \\ &- \mathbf{K}_{011}\boldsymbol{\eta} - \mathbf{K}_{012}\boldsymbol{\eta} \cos(\Omega_0 t) - \mathbf{K}_{013}\boldsymbol{\eta} \sin(\Omega_0 t) - \mathbf{C}_0\dot{\boldsymbol{\eta}}],\end{aligned} \tag{36}$$

where

$$\begin{aligned}&\mathbf{K}_{011} = \boldsymbol{\phi}^{\mathrm{T}}\mathbf{K}_{11}\boldsymbol{\phi}, \quad \mathbf{K}_{012} = \boldsymbol{\phi}^{\mathrm{T}}\mathbf{K}_{12}\boldsymbol{\phi}, \quad \mathbf{K}_{013} = \boldsymbol{\phi}^{T}\mathbf{K}_{13}\boldsymbol{\phi}, \\ &\mathbf{K}_{0\varepsilon 1} = \boldsymbol{\phi}^{\mathrm{T}}\mathbf{K}_{\varepsilon 1}\boldsymbol{\phi}, \quad \mathbf{K}_{0\varepsilon 2} = \boldsymbol{\phi}^{\mathrm{T}}\mathbf{K}_{\varepsilon 2}\boldsymbol{\phi}, \quad \mathbf{K}_{0\varepsilon 3} = \boldsymbol{\phi}^{\mathrm{T}}\mathbf{K}_{\varepsilon 3}\boldsymbol{\phi},\end{aligned}$$

$$\mathbf{K}_0 = \begin{bmatrix} \ddots & & \\ & \omega_r^2 & \\ & & \ddots \end{bmatrix}, \quad \mathbf{C}_0 = \begin{bmatrix} \ddots & & \\ & 2\xi_r\omega_r & \\ & & \ddots \end{bmatrix}, \quad \mathbf{F}_{0Dk} = \boldsymbol{\phi}^{\mathrm{T}}\mathbf{F}_{Dk}$$

and ξ_r and ω_r are, respectively, the damping ration and the natural frequency of the r-order mode of the system.

Definition. For a nonlinear system with multi-degrees-of-freedom, the frequency of each expanded term at the right side of the normal equation of the first-order approximate nonlinear system is defined as the frequent factor. If a frequent factor appears in more than one place or more than one time, only one frequent factor is counted, i.e. all the terms which are with the same frequent factor are considered as one term [3].

Using the method of multiple scales [11], the corresponding frequent factors of Eq. (36) can be obtained as:

$$\begin{cases} k\Omega_1, \quad (k \pm p)\Omega_1, \quad k\Omega_1 \pm \omega_r, \quad \omega_r \pm \omega_i, \\ \Omega_0, \quad \Omega_0 \pm \omega_r, \quad \Omega_0 \pm k\Omega_1, \quad \Omega_0 \pm (k \pm p)\Omega_1, \\ \Omega_0 \pm 2\omega_r, \quad \Omega_0 \pm (\omega_r \pm \omega_i), \quad \Omega_0 \pm (\omega_r \pm k\Omega_1), \end{cases} \tag{37}$$

where $r, i = 1, 2, \ldots, 24$; $k, p = 1, 2, \ldots, N$.

According to the theory of nonlinear vibration, some resonance phenomena will take place in the system under certain conditions:

(1) On condition that $k\Omega_1 \approx \omega_r$ or $(k \pm p)\Omega_1 \approx \omega_r$, the super-harmonic resonance will take place in the system.

(2) On condition that $\Omega_0 \approx \omega_r$, the primary resonance will take place in the system.

(3) On condition that $\Omega_0 - \omega_r \approx \omega_r$, namely $\Omega_0 \approx 2\omega_r$, the 1/2-order sub-harmonic resonance will take place in the system.

(4) On condition that $\Omega_0 - 2\omega_r \approx \omega_r$, namely $\Omega_0 \approx 3\omega_r$, the 1/3-order sub-harmonic resonance will take place in the system.

(5) On condition that $\Omega_0 \pm \omega_r \approx \omega_j$, or $\Omega_0 \pm (\omega_r \pm \omega_i) \approx \omega_j$, or $\Omega_0 \pm (\omega_r \pm k\Omega_1) \approx \omega_j$, or $\Omega_0 \pm k\Omega_1 \approx \omega_j$, the combination resonance will take place in the system.

(6) On condition that $\omega_r \pm \omega_i \approx \omega_j$, the internal resonance will take place.

(7) On condition that two types of the resonance take place in the same time, the multiple resonance of the system will take place in the system.

As analyzed above, the natural frequency ω_r of the system is determined by the structural parameters and the composite material parameters, and the frequency Ω_0 is determined by the synchronous rev of the motor, so the frequent factors shown in Eq. (37) are related to the structural parameters, the electromagnetic parameters and the composite material parameters. That is to say, not only the structural parameters, but also the electromagnetic parameters and the composite material parameters have significant effects on the nonlinear vibration of the system.

4. Example

In order to study the effects of the electromagnetic parameters and the material parameters on the motor–linkage mechanism system with links fabricated from three-dimensional braided composites, the four-bar linkage mechanism with 1-links (without consideration of the effect of the electromotor on the mechanism), the three-phase AC motor–four-bar linkage mechanism system with 1-links and the three-phase AC motor–four-bar linkage mechanism system with 2-links are analyzed, respectively.

(1) The parameters of the electromotor.
The type of electromotor is YS8024 and the parameters of the electromotor are as follows: the length of the iron core of the motor $L_{01} = 80\,\mathrm{mm}$, the inner diameter of the stator $D_1 = 75\,\mathrm{mm}$, the rated power $P_N = 0.75\,\mathrm{kW}$, the rated current $I_N = 3.48/2.01\,\mathrm{A}$, the rated voltage $V = 220/380\,\mathrm{V}$, the length of the even

air-gap $\delta_0 = 0.25\,\text{mm}$, the magnetic permeability coefficient of air $\mu_0 = 4\pi \times 10{-}7\,\text{H/M}$, the saturation $k_u = 1.2$, the number of the magnetic pole-pair of compounded magnetic field $p = 2$, the rated rev $n_N = 1440\,\text{rpm}$, the mass of the rotor $m_{10} = 2.93\,\text{kg}$, the moment of inertia of the rotor $J_{10} = 0.021\,\text{kg m}$, the frequency of the power supply $f = 50\,\text{Hz}$, the synchronous rev of the motor $\omega_0 = 25\,\text{Hz}$.

(2) The geometrical parameters of the four-bar linkage mechanism.
L, b and h, respectively, represent the length, width and thickness of the links; the cross-sectional parameters of every bar: $b = 20\,\text{mm}$, $h = 5\,\text{mm}$; the lengths are: crank $L_1 = 210\,\text{mm}$, coupler $L_2 = 585\,\text{mm}$, rocker $L_3 = 430\,\text{mm}$, and frame $L_4 = 600\,\text{mm}$.

(3) The material parameters of the 1-links fabricated from three-dimensional braided composites.
The material composition of the 1-links is T300 Epoxylite and the material parameters are taken as follows: G_{2m} is the shear elastic modulus of matrix, and $G_{2m} = 1.26\,\text{GPa}$; v_{2f} and v_{2m} are, respectively, the volume ratio of fiber and matrix, and $v_{2f} = 0.25$, $v_{2m} = 0.35$; ρ_{2f} and ρ_{2m} are, respectively the densities of fiber and matrix, and $\rho_{2f} = 1.76\,\text{g/cm}^3$, $\rho_{2m} = 1.36\,\text{g/cm}^3$; the total volume ratio of fiber is 0.6; α and β are the braided angles, and $\alpha = 30^\circ$, $\beta = 30^\circ$.

(4) The material parameters of the 2-links fabricated from three-dimensional braided composites.
The material composition of the 2-links is T300 Epoxylite too. The material parameters of the 2-links are the same as those of the 1-links except α and β, and $\alpha = 53^\circ$, $\beta = 47^\circ$.

It is assumed that the rotating speed of the crank is $\Omega_1 = 288\,\text{rev/min}$ (= 4.8 Hz), and it can be obtained by Eq. (24) that $\Omega_0 = 2\omega_0 = 50\,\text{Hz}$.

For the four-bar linkage mechanism with 1-links fabricated from three-dimensional braided composites (without consideration of the effect of the electromotor), the first three-order natural frequencies of the mechanism are calculated to be that $\omega_1 = 47\,\text{Hz}$, $\omega_2 = 153\,\text{Hz}$ and $\omega_3 = 269\,\text{Hz}$. According to the parameters above, we obtain $10\Omega_1 \approx \omega_1$, which shows that the condition of the super-harmonic resonance is satisfied, so the super-harmonic resonance of the mechanism will take place on condition that $10\Omega_1 \approx \omega_1$. Meantime, the forced vibrations of the mechanism will take place due to the self-excitation force, whose excitation frequencies are obtained as $\Omega_1, 2\Omega_1, \ldots, k\Omega_1$ by Eq. (32). The simulation time-domain and frequency-domain dynamic response characteristics curves of the coupler midpoint of the mechanism are shown in Figs. 8 and 9, respectively. In Fig. 9, it is known by analyzing that the peak at the first-order natural frequency ($\omega_1 = 47\,\text{Hz}$) is mainly caused by the super-harmonic resonance and the peaks at the lower frequencies are mainly caused by the forced vibrations.

For the three-phase AC motor–four-bar linkage mechanism system with 1-links fabricated from three-dimensional braided composites, the first three-order natural frequencies of the system are calculated to be that $\omega_1 = 47\,\text{Hz}$, $\omega_2 = 153\,\text{Hz}$ and $\omega_3 = 269\,\text{Hz}$. According to the parameters above, we obtain $\Omega_0 - \Omega_1 \approx \omega_1$ and $10\Omega_1 \approx \omega_1$, which show that the conditions of the combination resonance and the super-harmonic resonance are satisfied in the same time, so the multiple resonance of the system will take place on condition that $\Omega_0 - \Omega_1 \approx \omega_1$ and $10\Omega_1 \approx \omega_1$. Meantime, the forced vibration of the system will take place due to the self-excitation force, whose excitation frequencies are obtained as $\Omega_1, 2\Omega_1, \ldots, k\Omega_1$ by Eq. (32). The simulation time-domain and frequency-domain dynamic response characteristics curves of the coupler midpoint of the system are shown in Figs. 10 and 11, respectively. In Fig. 11, it is known by analyzing that the peak at the

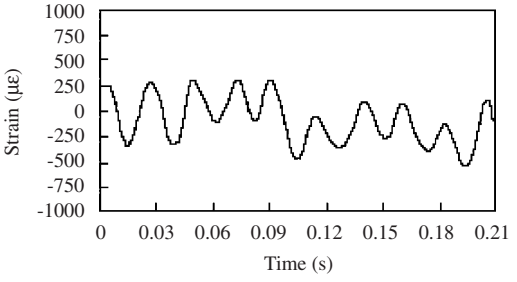

Fig. 8. Simulation time-domain dynamic response characteristics curve of the coupler midpoint.

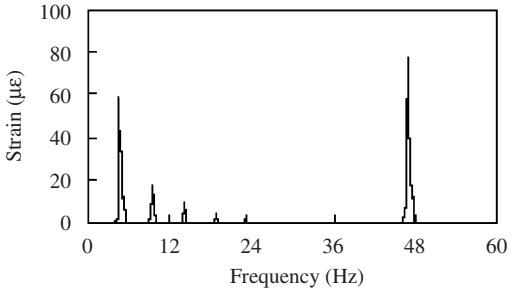

Fig. 9. Simulation frequency-domain dynamic response characteristics curve of the coupler midpoint.

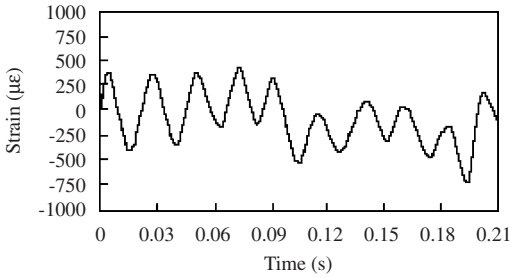

Fig. 10. Simulation time-domain dynamic response characteristics curve of the coupler midpoint.

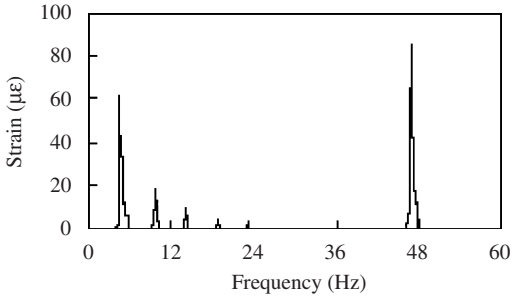

Fig. 11. Simulation frequency-domain dynamic response characteristics curve of the coupler midpoint.

first-order natural frequency ($\omega_1 = 47$ Hz) is mainly caused by the multiple resonance and the peaks at the lower frequencies are mainly caused by the forced vibrations.

For the three-phase AC motor–four-bar linkage mechanism system with 2-links fabricated from three-dimensional braided composites, the first three-order natural frequencies of the system are calculated to be that $\omega_1 = 47$ Hz, $\omega_2 = 177$ Hz and $\omega_3 = 313$ Hz. According to the parameters above, we obtain $\Omega_0 + \Omega_1 \approx \omega_1$ and $11\Omega_1 \approx \omega_1$, which show that the conditions of the combination resonance and the super-harmonic resonance are satisfied in the same time, so the multiple resonance of the system will take place on condition that $\Omega_0 + \Omega_1 \approx \omega_1$ and $11\Omega_1 \approx \omega_1$. Meantime, the forced vibration of the system will take place due to the self-excitation force, whose excitation frequencies are obtained as Ω_1, $2\Omega_1$, …, $k\Omega_1$ by Eq. (32). The simulation time-domain and frequency-domain dynamic response characteristics curves of the coupler midpoint of the system are shown in Figs. 12 and 13, respectively. In Fig. 13, it is known by analyzing that the peak at the first-order natural frequency ($\omega_1 = 54$ Hz) is mainly caused by the multiple resonance and the peaks at the lower frequencies are mainly caused by the forced vibrations.

The results of the simulations presented in Figs. 8–13 show: (1) the dynamic responses of the coupler midpoint of the system with consideration of the effect of the electromotor are greater than those of the system without consideration of the effect of the electromotor, because the electromagnetic parameters of the motor

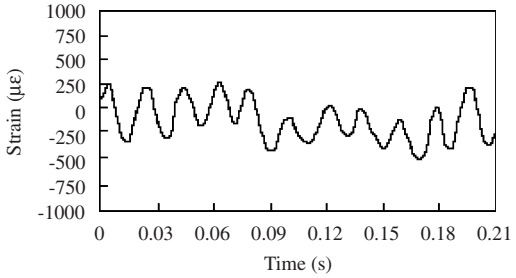

Fig. 12. Simulation time-domain dynamic response characteristics curve of the coupler midpoint.

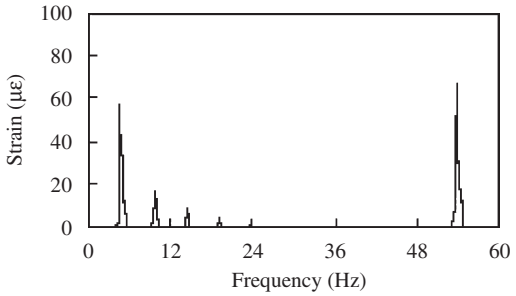

Fig. 13. Simulation frequency-domain dynamic response characteristics curve of the coupler midpoint.

have important effects on the nonlinear vibration of the system; (2) the dynamic responses of the coupler midpoint of the system vary with the material parameters of three-dimensional braided composites, because the material parameters have important effects on the nonlinear vibration of the system.

5. Conclusions

In this paper, the nonlinear vibration of the three-phase AC motor–linkage mechanism system with links fabricated from three-dimensional braided composite materials is studied. The relation between the nonlinear vibration of the system and the parameters of the system is obtained. The study shows that not only the structural parameters, but also the electromagnetic parameters and the material parameters have significant effects on the nonlinear vibration of the system; and that under certain conditions, there exist internal resonance, super-harmonic resonance, 1/2-order sub-harmonic resonance, 1/3-order sub-harmonic resonance, combination resonance, and multiple resonance. This paper is helpful for deeply carrying out the analytical and experimental studies on the dynamic response, harmonic oscillations, stability and choas control of the motor–linkage mechanism system with links fabricated from three-dimensional braided composite materials.

Acknowledgments

The research was supported by the National Natural Science Foundation of China under Grants 50175031. The support is gratefully acknowledged.

Appendix

According to the finite element method, $W_{1Y}(x, t)$, $W_{1Z}(x, t)$ and $V_1(x, t)$ can be expressed as

$$\begin{cases} W_{1Y}(x,t) = \phi_1(x)u_1(t), \\ W_{1Z}(x,t) = \phi_2(x)u_2(t), \\ V_1(x,t) = \sum_i \phi_i(x)u_i(t), \quad i = 3,4, \end{cases}$$

where $\phi_1(x)$, $\phi_2(x)$, $\phi_3(x)$, $\phi_4(x)$ are the shape functions, and

$$\phi_{1,2}(x)=\begin{cases}1-10e_{11}^3+15e_{11}^4-6e_{11}^5, & x\leqslant l_{11}\\ 1-10e_{12}^3+15e_{12}^4-6e_{12}^5, & l_{11}<x\leqslant l_{11}+l_{12}\\ 0, & l_{11}+l_{12}<x\leqslant l_{11}+l_{12}+l_{13}\end{cases}$$

$$\phi_3(x)=\begin{cases}0, & x\leqslant l_{11},\\ 1-e_{12}, & l_{11}<x\leqslant l_{11}+l_{12},\\ e_{13}, & l_{11}+l_{12}<x\leqslant l_{11}+l_{12}+l_{13},\end{cases}$$

$$\phi_4(x)=\begin{cases}0, & x\leqslant l_{11},\\ 0, & l_{11}<x\leqslant l_{11}+l_{12},\\ 1-e_{13}, & l_{11}+l_{12}<x\leqslant l_{11}+l_{12}+l_{13},\end{cases}$$

where $e_{11}=x/l_{11}$, $e_{12}=l_{11}+l_{12}-x/l_{12}$, $e_{13}=l_1-x/l_{13}$.

The mass matrix of the electromotor element $\bar{\mathbf{m}}_1$ is

$$(\bar{\mathbf{m}}_1)_{11}=\int_0^{l_1}[m_1(x)+m_{10}\delta(l_{11})]\phi_1(x)\phi_1(x)\,\mathrm{d}x,$$

$$(\bar{\mathbf{m}}_1)_{22}=\int_0^{l_1}[m_1(x)+m_{10}\delta(l_{11})]\phi_2(x)\phi_2(x)\,\mathrm{d}x,$$

$$(\bar{\mathbf{m}}_1)_{kp}=\int_0^{l_1}[J_1(x)+J_{10}]\phi_k(x)\phi_p(x)\,\mathrm{d}x, k,p=3,4,$$

the other terms of $\bar{\mathbf{m}}_1$ are zeros.

The stiffness matrix of the electromotor element $\bar{\mathbf{k}}_1$ is

$$(\bar{\mathbf{k}}_1)_{11}=\int_0^{l_1}E_1I_1(x)\left[\frac{\partial^2\phi_1(x)}{\partial x^2}\right]^2\mathrm{d}x,$$

$$(\bar{\mathbf{k}}_1)_{22}=\int_0^{l_1}E_1I_1(x)\left[\frac{\partial^2\phi_1(x)}{\partial x^2}\right]^2\mathrm{d}x,$$

$$(\bar{\mathbf{k}}_1)_{kp}=\int_0^{l_1}G_1J_{01}(x)\frac{\partial\phi_k(x)}{\partial x}\frac{\partial\phi_p(x)}{\partial x}\,\mathrm{d}x,\quad k,p=3,4.$$

The stiffness matrix of the electromotor element $\bar{\mathbf{k}}_{01}$ is

$$(\bar{\mathbf{k}}_{01})_{11}=-2g_4-g_5\cos(\Omega_0t)-g_6\sin(\Omega_0t),$$

$$(\bar{\mathbf{k}}_{01})_{12}=(\bar{\mathbf{k}}_0)_{21}=-g_5\sin(\Omega_0t)+g_6\cos(\Omega_0t),$$

$$(\bar{\mathbf{k}}_{01})_{22}=-2g_4+g_5\cos(\Omega_0t)+g_6\sin(\Omega_0t),$$

the other terms of $\bar{\mathbf{k}}_{01}$ are zeros, where

$$\Omega_0=2\omega_0,$$

$$g_4=\frac{\pi R_1L_{01}\Lambda_0}{4\sigma^2}[F_{1m}^2+F_{2m}^2+2F_{1m}F_{2m}\cos\phi],$$

$$g_5=\frac{\pi R_1L_{01}\Lambda_0}{4\sigma^2}[F_{1m}^2+F_{2m}^2\cos 2\phi+2F_{1m}F_{2m}\cos\phi],$$

$$g_6 = \frac{\pi R_1 L_{01} \Lambda_0}{4\sigma^2}[F_{2m}^2 \sin 2\phi + 2F_{1m}F_{2m} \sin \phi],$$

$\mathbf{K}_{11}$, $\mathbf{K}_{12}$ and $\mathbf{K}_{13}$ are:

$$(\mathbf{K}_{11})_{11} = (\mathbf{K}_{11})_{22} = -2g_4,$$

$$(\mathbf{K}_{12})_{11} = -g_5, \quad (\mathbf{K}_{12})_{12} = (\mathbf{K}_{12})_{21} = g_6, \quad (\mathbf{K}_{12})_{22} = g_5,$$

$$(\mathbf{K}_{13})_{11} = -g_6, \quad (\mathbf{K}_{13})_{12} = (\mathbf{K}_{13})_{21} = -g_5, \quad (\mathbf{K}_{13})_{22} = g_6,$$

the other terms of $\mathbf{K}_{11}$, $\mathbf{K}_{12}$ and $\mathbf{K}_{13}$ are zeros.

According to the finite element method, $W_2(\bar{x}, t)$ and $V_2(\bar{x}, t)$ can be expressed as

$$\begin{cases} W_2(\bar{x}, t) = \sum_i \phi_i(\bar{x}) u_i(t), & i = 6, 7, 8, 10, 11, 12, \\ V_2(\bar{x}, t) = \sum_j \phi_j(\bar{x}) u_j(t), & j = 5, 9, \end{cases}$$

where $\phi_5(\bar{x})$, $\phi_6(\bar{x})$, $\phi_7(\bar{x})$, $\phi_8(\bar{x})$, $\phi_9(\bar{x})$, $\phi_{10}(\bar{x})$, $\phi_{11}(\bar{x})$, $\phi_{12}(\bar{x})$ are the shape functions, and

$$\phi_5(\bar{x}) = 1 - e_2,$$

$$\phi_6(\bar{x}) = 1 - 10e_2^3 + 15e_2^4 - 6e_2^5,$$

$$\phi_7(\bar{x}) = l_2(e_2 - 6e_2^3 + 8e_2^4 - 3e_2^5),$$

$$\phi_8(\bar{x}) = l_2^2(e_2^2 - 3e_2^3 + 3e_2^4 - e_2^5)/2,$$

$$\phi_9(\bar{x}) = e_2,$$

$$\phi_{10}(\bar{x}) = 10e_2^3 - 15e_2^4 + 6e_2^5,$$

$$\phi_{11}(\bar{x}) = l_2(-4e_2^3 + 7e_2^4 - 3e_2^5),$$

$$\phi_{12}(\bar{x}) = l_2^2(e_2^3 - 2e_2^4 + e_2^5)/2,$$

where $e_2 = \bar{x}/l_2$.

The mass matrix of the beam element $\bar{\mathbf{m}}_2$ is

$$(\bar{\mathbf{m}}_2)_{ij} = \int_0^{l_2} \rho_2 A_2(\bar{x}) \phi_i(\bar{x}) \phi_j(\bar{x}) \, \mathrm{d}\bar{x}, \quad i, j = 6, 7, 8, 10, 11, 12,$$

$$(\bar{\mathbf{m}}_2)_{kp} = \int_0^{l_2} \rho_2 A_2(\bar{x}) \phi_k(\bar{x}) \phi_p(\bar{x}) \, \mathrm{d}\bar{x}, \quad k, p = 5, 9.$$

The stiffness matrix of the beam element $\bar{\mathbf{k}}_2$ is

$$\bar{\mathbf{k}}_2 = \sum_{j=1}^{4} \frac{1}{2} \int_{\Omega_j} S_2^{\mathrm{T}} L_{2j}^{\mathrm{T}} C_{2j} L_{2j} S_2 \, \mathrm{d}\Omega_j.$$

References

[1] J. Chunmei, Q. Yang, F. Ling, Z. Ling, The non-linear dynamic behavior of an elastic linkage mechanism with clearances, *Journal of Sound and Vibration* 249 (2002) 213–226.

[2] L.D. Seneviratne, S.W.E. Earles, Chaotic behaviour exhibited during contact loss in clearance joint of four-bar mechanism, *Mechanism and Machine Theory* 27 (1992) 307–321.

[3] Y.X. Wang, Multifrequency resonances of flexible linkages, *Mechanism and Machine Theory* 33 (1997) 255–271.

[4] S.R. Hsieh, S.W. Shaw, The dynamic stability and non-linear resonance of a flexible connecting rod: single-mode model, *Journal of Sound and Vibration* 170 (1994) 25–217.
[5] H.Z. Liu, J.P. Wang, Z.M. Zhang, Strain-dependent nonlinear damping and application to dynamic analysis of elastic linkage mechanism, *Journal of Sound and Vibration* 281 (2005) 399–408.
[6] G.W. Du, F.K. Ko, Unit cell geometry of 3-D braided structure, *Proceeding of ASC Sixth Technical Conference*, Albany, NY, October 1991, pp. 6–9.
[7] J.M. Yang, C.L. Ma, T.W. Chou, Fiber inclination model of three-dimensional textile structural composites, *Journal of Composites* 20 (1986) 472–483.
[8] G.W. Cai, The design of flexible linkage mechanisms fabricated from three-dimensional braided composite with optimal link properties, *International Conference on Mechanical Transmissions and Mechanisms* (1997) 405–409.
[9] J.J. Qiu, *Electromechanical Analytical Dynamics*, Science Press, Beijing, 1997.
[10] C. Zhang, *Analysis and Design of Elastic Linkage Mechanism*, China Machine Press, Beijing, 1997.
[11] J.M.T. Thompson, H.B. Stewart, *Nonlinear Dynamics and Chaos*, Wiley, New York, 1986.